Utrecht University

Faculteit Bètawetenschappen

Bachelor Thesis

Physics and Astronomy

Charm particle production in High Energy Cosmic Ray Showers using CORSIKA simulations

Author:
Peter Gaemers

Supervisors:
Dr. Alessandro Grelli

Dr. André Mischke

Institute for Subatomic Physics

January 13, 2016

Abstract

Cosmic Ray Showers have been an active area of research ever since their first discovery. Until resently simulations where unable to include heavy quarks as a part of the shower. In this thesis I research the influence of the charm quark on the transverse momentum distribution of muons, electrons, photons and neutrino's for various primairy particle energies using the CORSIKA simulation program. From this we can calculate the ratio of the muon momenta to photon+electron momenta. Using the HiSparc project this ratio can be determained from observed data. If charm particles have an effect on this ratio the HiSparc project can observe this.

Contents

Chapter 1

Introduction

In the course of the last 100 years the discovery of and research in Cosmic Rays have increased our knowledge of their nature and origin while also contributing significantly to particle physics in general. Although accelerators like the Large Hadron Collider (LHC) are now the dominant player in particle physics research, the research of cosmic rays have one advantage over the current particle accelerators. The energy of Cosmic Rays goes up to 10^{20} electron Volt (eV), dwarfing the 10^{13} eV where the accelerators are doing their job.

The clear description of particle interactions in this energy range is lacking. One of the processes often neglected in the shower of particles created by a high energy cosmic ray is the production and interactions of heavy quarks with the atmosphere. If the incoming cosmic ray has high enough energy the heavy quarks produced in the aftermath will be energetic enough to have a decay length long enough for them to interact with their surroundings rather then decay straight away. The higher mass of particles containing a charm quark leads to a on average higher elastisity in interactions then lighter particles. This has an effect on the development of the resulting Extensive Air Shower which is produced as a result of the colliding cosmic ray. It is expected that charm particles lead to higher momenta and number of particles resulting from air showers. In my research I shall investigate the influence of the Charm quark in these high energy interactions. Using the Monte Carlo simulation program CORSIKA, COsmic Ray SImulator for KAscade, I investigate the effect of charm particles on the transverse momentum distribution of photons, electrons, muons and neutrino's for various energies for the primairy cosmic ray particle. This should lead to an observable shift in the data collected by the HiSparc project. HiSparc is a project of universities and highschools for studying cosmic rays using scintillator detectors. The signal produced by a detector is proportional to the momenta of the particle going through. With charm included it should lead to better agreement between the detected signals and simulations of cosmic rays.

Chapter 2

Cosmic Ray Showers

2.1 History

As is not uncommon in physics, the discovery of Cosmic Rays happened accidentally. After the discovery of radioactivity in 1896 by Marie Curie and Henry Becquerel it was believed the ionization of air was caused by radioactive decay of elements in the ground. It was Theodure Wulf who in 1909 devoloped an electrometer with which he could measure the ionization rate. He expected to be able to measure a decrease in ionization rate with increasing altitude. Using the electrometer at the top of the Eiffel tower he actually showed the level of radiation went up with increasing altitude.

Figure 2.1: Victor Hess prepairing for his balloon flight. Source: *http* : *//faculty.washington.edu/wilkes/salta/hess.gif*

A more definitive answer of what caused this radiation was given by Victor Hess in 1912. He first perfected the electrometer and during the course of 1911 and 1912 took several ballon flights. With his measurements he showed a decrease at lower altituded up to around 1000 meters. To his surprise above this alititude the radiation intensified until reaching doule intensity at 5000 meter above sea level. There was no variation in radiation during the day, not even during a solar eclips. Based on this Hess ruled out the sun as a possible

source, concluding there is some kind of high energy radiation entering Earth's atmosphere from space.

Hess continued his investigations with more precise measurements showing a very small daily variation. At the same time Compton's theoretical work showed these variations where consistent with the impact of the rotation of the Milkyway galaxy on Earth's motion. They concluded the observed radiation to be from stellar systems far beyond our own galaxy.

2.2 Energy Spectrum

The Energy spectrum of cosmic rays extends from 10^6 eV to 10^{20} eV with primairy particles including all stable nuclei, charged particles and some unstable particles with a large lifetime.

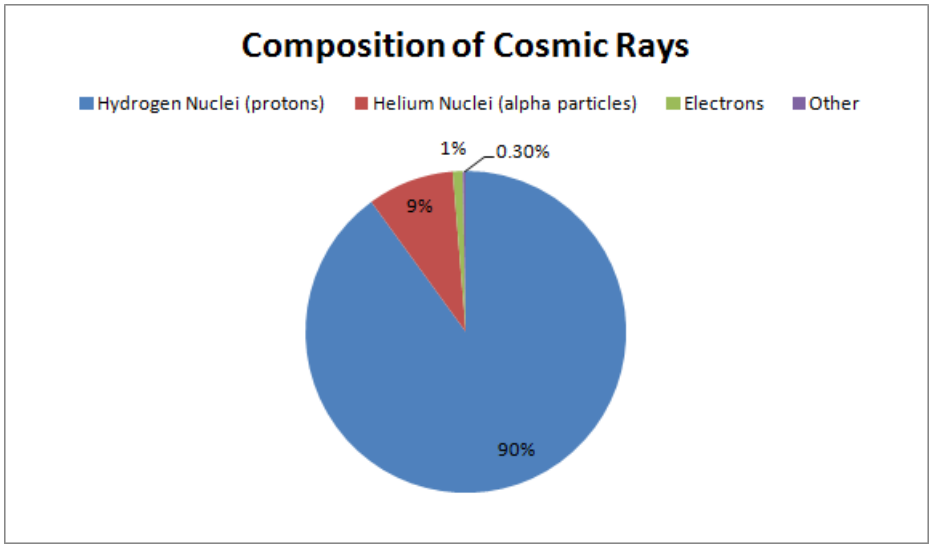

Figure 2.2: Composition of Cosmic rays. Source: *http* : *//2.bp.blogspot.com/* − *fd9LVAMtjbE/U0kmmyZmkkI/AAAAAAAAAzk/KCQtTcg7Jvk/s*1600*/Composition*+ *of* + *Cosmic* + *Rays.png*

As is depicted in the figure above the vast majority of cosmic rays are protons, making up 90 percent of all cosmic rays. Next is Helium making up 9 percent.

The energy spectrum has been determained by a large number of experiments. The flux fall off as a function of energy, following a power law:

$$\Phi(E) \propto E^{-\gamma}$$

γ is called the spectral index. The flux decreases from 1000 particles per second per m^2 around the 10^9 eV to less than 1 particle per century around the 10^{20} eV.

It is mainly featureless with only two clear transition points, the knee at 10^{15} eV and the ankle at 10^{19} eV. This gives rise to 3 energy intervals, with

different values for γ. This is illustrated in Fig 2.3. These different regions are due to different mechanisms responsible for the acceleration of the particles.

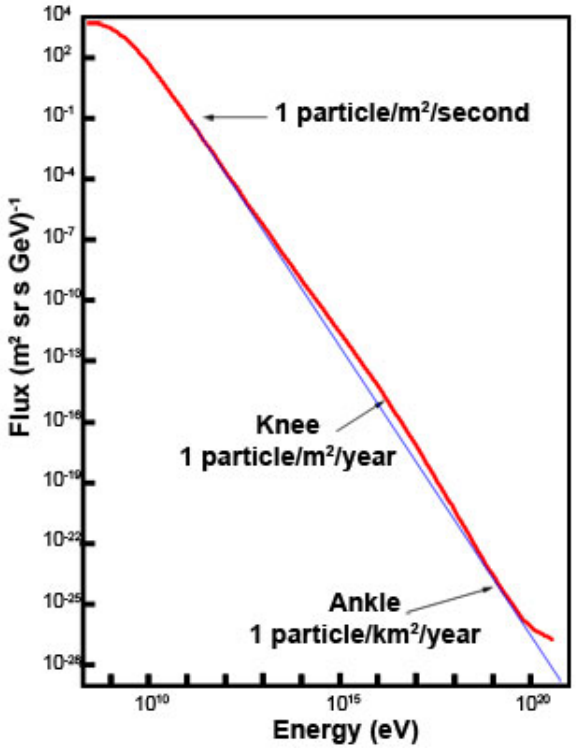

Figure 2.3: The flux of cosmic rays as a function of energy. The points where the spectral index changes, the knee and ankle are marked. Source:

The first part of the spectrum has $\gamma \approx 2.7$. The lowest energy cosmic rays are produced in the sun from events like solar flares. The higher end of this part of the spectrum is due to interstellar gas being ionized by solar radiation and than being accelerated by repeted collision with a shock wave in the solar wind. This is called the Fermi mechanism. The maximum energies achievable are around 10^{10} eV. The higher energy cosmic rays are expected to be originating from supernova remnants. The basic idea is the same as in the solar wind. Particles are accelerated by colliding with shockwaves. Due to strong magnetic fields the particles are deflected causing multiple collisions with the shockwave, gaining energy every time until the particle escapes. The upper limit for this energy using an average Type II supernovae is around 10^{14} eV.

At the knee the spectral index changes to $\gamma \approx 3.1$. The change in flux around the knee is due to a decrease in flux from light nuclei, namely proton and helium. The proton flux has a distrinct break around $4 * 10^{15}$ eV and so does the Helium flux at a slightly higher energy.

Exact explanations for this are still unknown, although most likely this is due to a maximum in achieveable energy from the source and leakage from galaxies in the propagation process. Between the knee and the ankle extragalactic particles come into play. Due to lack of understanding of the interstellar medium

the origin and the acceleration mechanism of these particles in not understood. Bottom-up scenaries assume high energy particles to come from low energy particles accelerated at their source, based on the Fermi mechanism and due to acceleration in intense electric fields. Top-down scenarios assume high energy particles to be produced by the decay of super massive unstable particles. However this would also lead to a very large fraction of the high energy particles beeing produced to be photons which is dismissed by observations.

Last important feature is the ankle. At energies around $10^{19.5}$ eV there is a suppression of the spectrum due to interactions with the Cosmic Microwave Background. This was first predicted by Greisen, Zatsepin and Kuzmin and is called the GZK cut-off. When a cosmic ray of such high energy has a collision with a CMB photon the availible energy is large enough for pion production. This interaction causes the cosmic ray to lose energy until it falls below the threshold of $5 * 10^{19}$ eV. The result is a pile up of cosmic rays with energies just below this and is why the flux slope flattens out.

The mean free path of such protons is around 10^6 parsec. If cosmic rays with higher energies are observed this means they have to have travelled less then approximatly 50 Mpc. So if this limit is observed or not points to the distance of the cosmic ray sources.

2.3 Extensive Air Showers

Upon arrival at the Earth's atmosphere the cosmic rays interacted inelastically with atmospheric nuclei. At these collisions a large amount of secondary particles are being produced, mainly photons, electrons and pions. The basic idea is illustrated in figure 2.4. A incoming proton collides with air and as a result more different particles are produced.

These particles then also interact with the atmosphere causing more particles being produced. The then produced particle cascade is refered to as an Extensive Air Shower (EAS). This is the only way to observe high energy cosmic rays due to their low flux. The shower consists of three components: Electromagnetic, Hadronic and Muonic.

Figure 2.4 shows the EAS development of shower initiated by a proton, Helium and Iron nucleus with an energy of 10^{13} eV at a height of 30 kilometer above sea level. The different colors refer to the different components of the shower. Red for electromagnetic, blue for hadronic and green for muonic. The figure is made with CORSIKA using the PLOTSH option. More on this is in Chapter 4

The cascade is initiated by a hadronic interaction between the primairy particle and an atmospheric nucleus.

Here a large amount of photons, electrons and positrons are produced forming the largest part of the electromagnetic component. This component loses energy mainly due to Bremsstrahlung and pair production. This lowers the average energy of the particles until it becomes low enough for ionization to play a role which slowly absorbs the shower.

At the first interaction also hadrons are produced, mostly charged and neutral pions. Neutral pions decay into photons, feeding smaller electromagnetic showers. Charged pions either interact and feed the hadronic component, or decay into muons and neutrino's. The Electomagnetic component does not vary

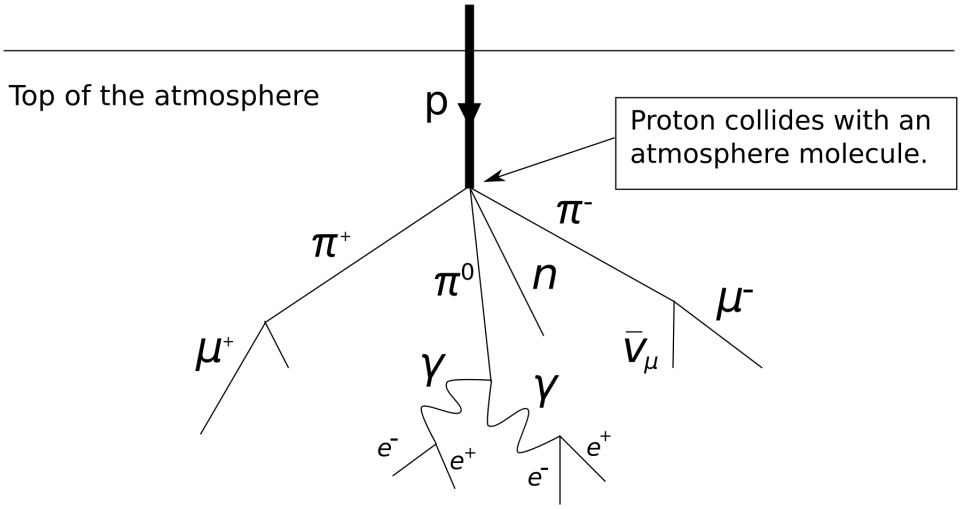

Figure 2.4: Schematic view of a Cosmic ray collision leading to the formation of an EAS. Source: *https* : *//upload.wikimedia.org/wikipedia/commons/thumb/0/08/Atmospheric*$_C$*ollision.svg/2000px−Atmospheric*$_C$*ollision.svg.png*

much for different primairy particles. A heavy primairy particle does produce significantly more muons.

2.4 Heavy Quarks

Due to the high energy of some EAS it is possible for heavy quarks to be produced. The heavy quarks being charm, bottom and top. Here I only focus on the charm quark. With increasing energy the lifetime, and thus also decay length, of these particles increases due to time dilation from the Special Theory of Relativity. Above a certain critical energy, which for charm particles in expected to be 10^{16}eV, the decay probability of these particles decreases rapidly leading to decay lengths of kilometers. This allowes the heavy particles to interact with atmospheric particles before decaying. Because of their high mass, charmed particles have on average a higher elasticity when colliding with the atmosphere. This couses a higher fraction of the primairy particle energy to be transported to greater depth.

For an EAS this would mean if charm particles are present in the early stage of the shower the development of the shower would be delayed to larger depths. This results in a higher number of particles being produced at larger depths, with higher momentum.

2.5 Observational methodes

Observational methodes of Cosmic rays can be divided into two catagories: direct and indirect. Direct methodes aim to directly observe the incomming

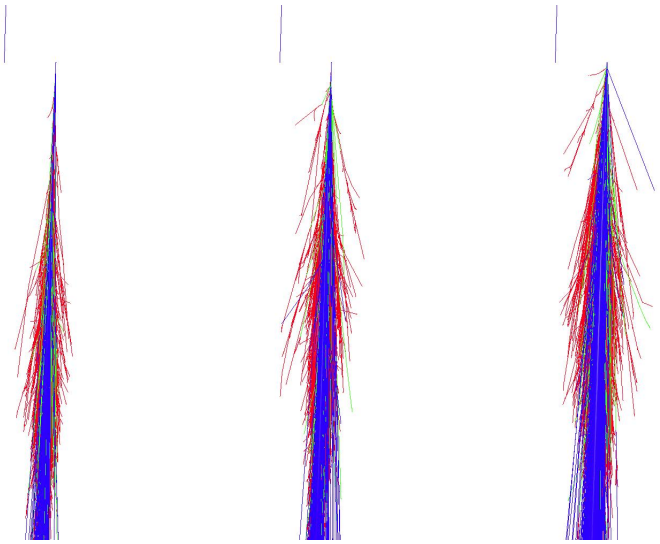

Figure 2.5: Longitudinal development of, from left to right, a proton, helium and iron colliding with an atmospheric oxygen atom at a height of 30 kilometers with a primairy particle energy of 10^{11} eV.

primairy particles. This is mainly done by satallite. Indirect methodes are focused on the detection in the secondairy particle showers.

- Water Cherenkov tank A Water Cherenkov Tank is a sealed tank filled with water. Due to the refractive index of water the speed of light is lower in water then in the vacuum. This makes it possible for a particle to go through water with a speed higher then the speed of light. When this happens a special kind of light is emitted by the particle, called Cherenkov radiation. This light can be captured by photomultipliers and the direction of motion of the charged particles can be observed. This provides information of the direction and the number of particles in the EAS.

- Air Fluorescence Detectors This detectors focuses on the light emitted by atmospheric nitrogen after its interaction with a charged particle in the atmosphere, giving a detailed information of the development of the showers in the atmosphere. However data can only be taken with this techniek under high quality atmospheric and environmental conditions.

  The Pierre Auger Observatory in Argentia is an air shower experiment using both a water cherenkov and air fluorence detector. This Observatory has 1660 water tanks and 24 telescopes.

- Scintillator detector A scintillator is a plate of plastic material which emits light when a charged particle goes through it. This light is then captured by a phtotmultiplier converting the light into an electronic signal. From this signal the energy of the particle going through the detector can be deterement. This is the type of detector used by the HiSparc project.

- Low frequenty radio detectors Just as light is emitted by the atmosphere when high energy particles goes through it, radio waves are also emitted.

With radio detectors this can be measured. A large advantage of this over Air Fluorence detectors is it can operate continiously. If triggered by HiSparc the LOFAR observatory can be used to search for air showers.

Chapter 3

HiSparc

3.1 What is HiSparc

HiSparc (High School Project on Astrophysics Research with Cosmics) is a network of Cosmic Ray Shower detectors spread over multiple countries. Most of the stations are constructed, installed and financed by High Schools. The idea of HiSparc is the detection and reconstruction of EAS in the energy range above 10^{16} eV, so the high end of the Cosmic ray spectrum. Clusters of detectors are built around a university. Distances between different stations within a cluster vary between hundreds to thousands of meters. Due to the large distance between the clusters HiSparc is very well suited to study long-range correlations between cosmic ray showers.

3.2 Experimental Setup

Every station has 2 scintillator detectors and a GPS antenna. Figure 3.1 gives a schematic view of the detector setup. The scintillators are connected to a photomultiplier, PMT. The signal is amplified and integrated. This is so it will fall of slower. Each PMT is connected to an 12 bit Analogue-Digital converter with two cables, one for power and controle, the other for the analoge signal. The signal from the PMT is sampled at 400 MHz. This gives a single event the maximum time window of 10 μs. When signals from both detectors pass the threshold within 2 μs the electronics store the samples from 2.44 μs before till 3.6 μs after the trigger is generated. the signals are stored and connected to the information from the GPS antenna. This is for an accurate time stamp. LaBVIEW is used for analyzing data en cotrolling the software.

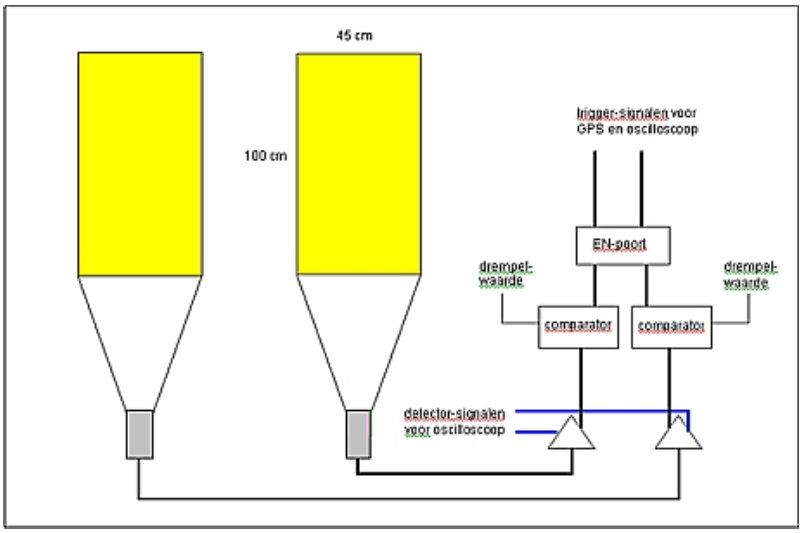

Figure 3.1: Schematic view of a HiSparc detector station. Source: *http* : *//www.fisme.science.uu.nl/hisparc/images/project*$_h$*isparc*$_s$*chema.jpg*

The individual detectors are placed in skyboxes and are positioned 5 to 10 meters apart.

Figure 3.2: Example of HiSparc detector setup on the roof of a high school. Source: *http : //www.ru.nl/publish/pages/*542007/*skiboxen − op − dak − school.jpg*

One scintillator cannot tell the difference between charged particles from an EAS and regular charged particles. When detecting coincident signals using two detectors a few meters apart the probablity of the particles beeing uncorrelated in reduced significantly. The dominant reason for coincident particles is them being part of the same EAS. With this set up an EAS with a primairy particle energy of 10^{17} eV can be detected with a core distance of up to 200 meters.

3.3 Pulse-height spectrum

The data looks like fig 3.3. It has two distinct features. At the left side of the spectrum there are large number of events with a low pulse-height. This peak is the signal due to high energy photons and electrons passing through the detector. This part of the signal follows an exponential decay. Further to the right is the second peak with a lower amount of events and a higher pulseheight. This is due to muons passing through the detector. They are describable with a Landau distribution. This is a narrow distribution with a long tail.

With this information we can fit these two functions on a dataset. Then we can integrate both fits and determain the ratio $Landau/Exponential$ which gives some numbers. This ratio is important because we can compare this to my simulation data. From the simulation data we can integrate the momenta

of photons+electrons and of the muons. The ratio of these two should be the same as from the experimental data.

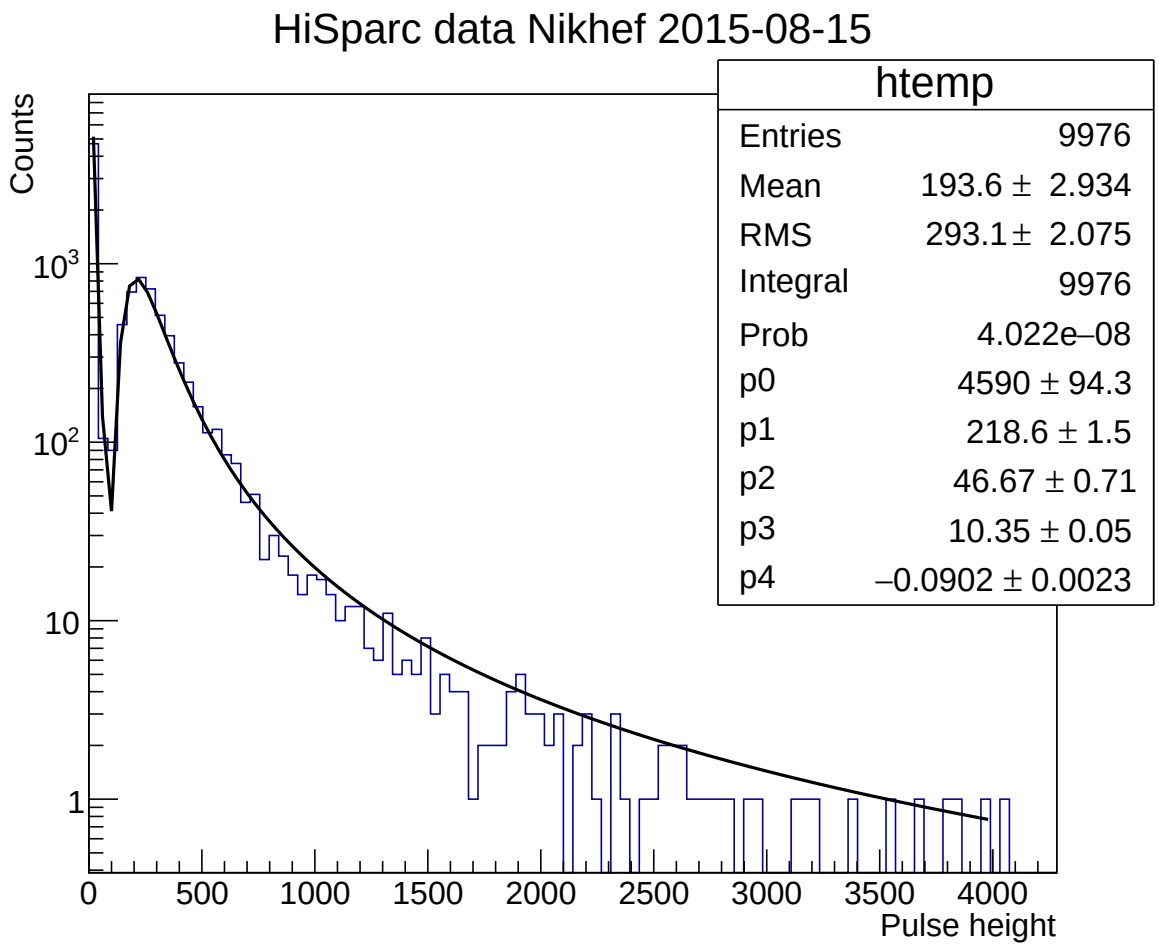

Figure 3.3: Fit of HiSparc data with a Landau and exponential. p0 to p2 refer to parameters of the Landau, the constant, most propabele value and sigma. p3 and p4 are the constant and slope of the exponential. For this dataset the ratio is 0.61

Chapter 4

Corsika

4.1 What is Corsika

To correctly analyze experimental data from EAS a detailed theoretical model of the development of the cascade is required. For this all knowledge of high energy interactions are required in Monte Carlo simulations. CORSIKA, COsmic Ray SImulations for KAscade, is a Monte Carlo program for studying the evolution of EAS generated by incoming Cosmic Rays. Using FORTRAN routines CORSIKA is able to simulate interactions and decays of particles produced by an EAS with a primairy energy of up to 10^{20} eV. It consists of four basic parts. The first is the general framework of the program and the tracking of particles in the atmosphere as well as performing decays of unstable particles. The second part handels high energy interactions with the atmosphere. The third part is in charge of low energy interactions while the fourth part simulates the behavior of photons, electrons and positrons.

A serious problem in simulating EAS is the extrapolation of hadronic interactions to energies much larger then covered by experimental data. Also the most energetic particles have an extreme forward direction which isn't accessible by collider experiments. So there must be relied on extrapolation of theoretical models. Multiple different interaction models are availible for this.

4.2 Used options

There is a variety of possible interaction models and options availible to use in simulation with CORSIKA. The ones I used are:

- QGSJET

  This is used for the high energy hadronic interactions. It's based on the Lund string model.

- GHEISHA

  This is used for interactions with Elab<= 80 GeV. It treats elastic and inelastic interactions and slow neutron capture based on experimental data.

- ROOTOUT

  Required to generate file output as a root tree, making analysis with ROOT possible.

- EHISTORY, MUADDI

  With this additional information about the prehistory of electromagetic and muonic particles is saved, leading to identification of mother and grandmother particles.

- NEUTRINO

  By default CORSIKA completely ignores neutrino's. Due to their low interaction cross sections they aren't expected to interact at all with the atmosphere so they don't contribute to the development of the EAS. With this option neutrino's are being produced by leptonic decay, while maintaining the assumption of no interactions with the atmosphere.

- CHARM This option is required for the production and propagation of charmed hadrons. Without this option produced charmed particles are not treated explicitly and decay at the vertex without being transported to CORSIKA.

- PLOTSH With this option the start and end points of all particle tracks are written out in seperate files for the electromagnetic, muonic and hadronic components. Together with the program *plottracks* plots of the longitudinal development can be made. Because this option results in extreamly large data outputs I only used this when making figure 2.3

4.3 Modifications to source code

In order for the CORSIKA to properly propagate charmed particles a modification to the qgsjet01d.f file is required in addition to the charm option. In the subroutine XXASET the cross sections for dealing with charm fragmentation need a non zero value. However by default this value is already non zero. So in order to make a clear distinction between shower with and without charm I've manually set the crosssection to zero when I want to exclude charm particles being produced and using their deault value when wanting charm particles to participate in the shower.

c Parameters for the soft fragmentation:
c DC(i) - relative probabilities for udu d (i=1), ss (i=2), cc (i=3)-pairs creation
c from the vacuum for the quark (u,d,u ,d) fragmentation; c ss (i=4), cc (i=5) - for the diquark (ud, u d) fragmentation
DC(1)=.06$D0$
DC(2)=.10$D0$
* DC(3)=.0003$D0$! To switch off charmed particles set to 0.000
DC(3)=.000$D0$
DC(4)=.36$D0$
* DC(5)=.001$d0$! To switch off charmed particles set to 0.000
DC(5)=.0$D0$

The values for DC(3) and DC(5) where $0.000d0$ in case of no charm and $0.0003D0$ and $0.001D0$ when charm was included. These values need to be changed before compiling CORSIKA with the desired options

4.4 Data keywords

For steering the simulation CORSIKA needs multiple Data keywords with values for parameters. I used most of the default settings. Here I'll list the ones I varied while the others are readable in the appendix.

- RUNNR 00702
- NSHOW 5 How many showers should be generated. Is this case 5
- PRMPAR 14 Specifying the primairy particle. This is set to a proton.
- ERANGE $1.E7$ Energy range of the primairy particle.
- OBSLEV The observation level was set to 0.
- FIXHEI1000002 Height in cm and particle of first interaction. 2 is an oxygen nucleus.
- SIGMAQ 0000 This is used to determain the interaction cross section of 1)charmed meson, 2)charmed baryon, 3)bottom mesons, 4)bottom baryons. With setting these values to 0 CORSIKA assigns the value using the parametrization which is discussed in the next section.
- PROPAQ 1 Selecting the routine to be used for the interactions of charmed particles. Setting this to 1 selects the PYTHIA routine for this. This keyword is only useable with the CHARM option.

4.5 Charm treatment

Charm particles are produced in QGSJET via soft fragmentation. In this process a c cbar pair is formed from the vacuum and coupled to quarks of hadronizing strings. The cross section of this process increases with higher energy from $\sigma = 39$ μb at $E_{lab} = 10^{10}$eV to $\sigma = 24$mb at $E_{lab} = 10^{20}$ eV. Another contribution comes from leading nucleon conversion into a leading Λ_c D pair. The crossesction for this varies from $\sigma = 25$ μ b at $E_{lab} = 10^{10}$eV to $\sigma = 310\mu$ b at $E_{lab} = 10^{20}$ eV. So at higher energies the contribution of this process becomes less and less important as the energy of the interaction increases.

To describe the interactions it is assumed the heavy bayrons and mesons transform into lighter charmed particles. For the bayrons they are all assumed to rapidly decay into Λ_c. The Λ_c then propagates through the atmosphere. The charm mesons are all assumed to decay to a D-meson.

Λ_c cross section is representative for all charm baryon interactions. In the same way the D-meson cross section is used for all mesons. The cross section in millibarn (mb) is then calculated with a parametrisation.

$\sigma^{H-air}(mb) = (1 - 4\sigma_{45}^2)p_0 + \sigma_{45}(2\sigma_{45} - 1)p_1 + \sigma_{45}(2\sigma_{45} + 1)p_2$

$\sigma_{45} = (\sigma^{H-p}[mb] - 45mb)/30$

$p_0 = 309.4268$ mb
$p_1 = 245.0771$ mb
$p_2 = 361.8057$ mb
With these cross sections the interaction length can be calculated as follows:
$\lambda_{int} = m_{air}/\sigma^{H-air}$

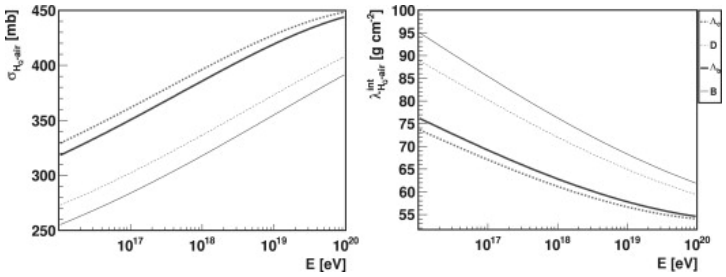

Figure 4.1: On the left is the resulting interaction cross section. On the right is the interaction length [2]

Figure 4.1 shows the resulting cross sections and interaction lengths for the Λ_c and D-meson.

The interactions of charm with the Earth's atmossphere is not included in QGSJET. For this linking with PYTHIA is required. In PYTHIA there are two different types of hadron-nucleus interactions, either partonic of diffractive.

In a partonic interaction the two hadrons exchange gluons. In a diffractive interaction the two colliding hadrons exchange momentum as a whole. The total inelastic cross section is the sum of the two. When interaction first the number of particles participating in the interaction has to determained. Each of these nucleons has a probability of having a diffractive interaction. The interaction is only considered diffractive as a whole when all interaction nucleons have a diffractive interaction. If not all but one of the remaining nucleons are split into quark-diquark pairs. Then the same amount of pairs are generated in the projectile with total energy E_{qqbar}. Then the partonic interaction between the projectile with an energy E_H-E_{qqbar} and the target nucleon takes place. Lastly quark- antiquark pairs are matched with quark- diquark pairs and hadronization takes place.

Chapter 5

Simulations

5.1 Simulations

For my analysis I have made two different sets of simulations.

The first set is to get an idea of the general look of a EAS for different energies. This set consists of 4 showers of 4 different energies, so one per energy. The energies used are 10^{14}, 10^{15}, 10^{16} and 10^{17} eV of the primairy particle. For these simulations the charm fragmentation cross sections are 0 and the CHARM option of CORSIKA is off.

Using the data from these simulations I will study the distribution in the x-y plane, the momentum distribution of muons, photons+electrons and neutrino's. And finally the different types of particles being produced and relative aboundancies..

The second set is to be able to see the influence of Charmed particles in the EAS. For this set I have made simulations of5 different energies, from 10^{14} and 10^{18} eV. The number of showers for every energy level varies. This contraint is due to the amount of data produced by simulation of a high energy shower being too large for the computer to store.

Energy(eV)	Number of showers
10^{14}	500
10^{15}	200
10^{16}	100
10^{17}	50
10^{18}	10

Table 5.1: Number of showers

This set has been done twice, once with the charm fragmentation cross sections as 0 and the CHARM option off, and once with the charm fragmentation cross sections as mentioned in the previous chapter and the CHARM option of CORSIKA on.

5.2 General Description

In Fig 5.1 the x-y coordinates of the particles reaching the observation level are plotted. It is immediately visible that the area covered by an EAS is much larger for a higher energy primairy particle. The average values for x and y as of the root mean squared of x and y do not vary so much. This indicates that even though the size of the shower increases drasticly, the majority of the particles are still contained in a relativly small area. In the Appendix are plots with the x-y distribution of Photons and electrons, muons and neutrino's.

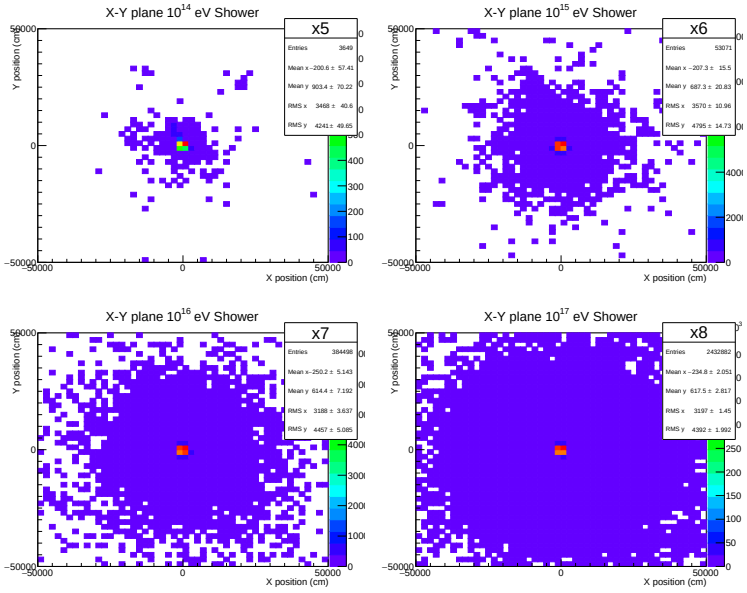

Figure 5.1: x-y distribution for showers with different primairy particle energies

In Fig 5.2 the momentum distribution of Muons, Photons+electrons and Neutrino's are plotted. Different color are used for different energy of the primairy particle. Blue is 10^{14} eV, red is 10^{15} eV, teal is 10^{16} eV and green is 10^{17} eV, For the momentum distributions the same few things happen in all three histograms. Namely the number of particles for every species goes up and there is a slight shift towards higher energy. Also the tail of the distributions grow much larger at higher energy.

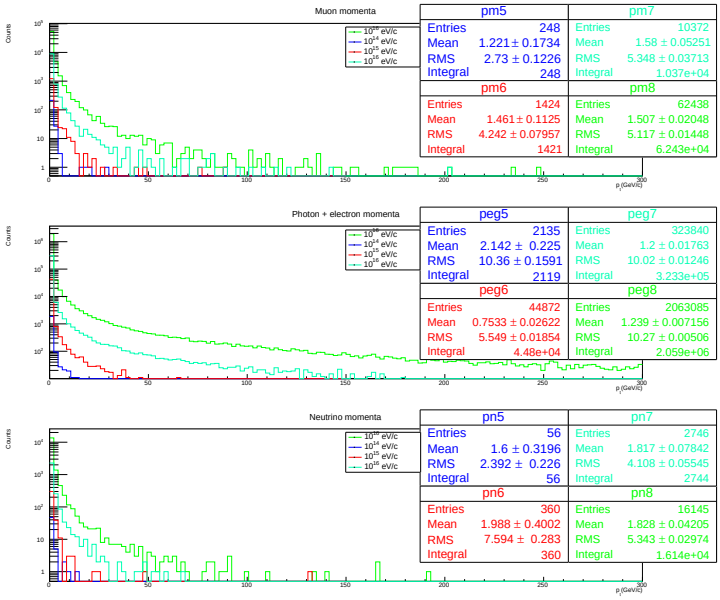

Figure 5.2: Momentum distribution of photons, electrons, muons and neutrino's for showers with energies 10^{14}, 10^{15}, 10^{16}, 10^{17}.

Lastly the different types of particles. In Fig 5.3 the relative aboundancies of the different particles are shown for the 4 different energies. In table 5.2 is the legend which number refers to which type of particle.

What stands out is the fact that the histograms look every similar for different energies. The relative aboundancies of the different species of particles doesn't seem to change very much as a function of energy. What does change very much is the total amount of particles being produced in the showers.

Figure 5.3: 10^5 Relative aboundancies of different types of particles.

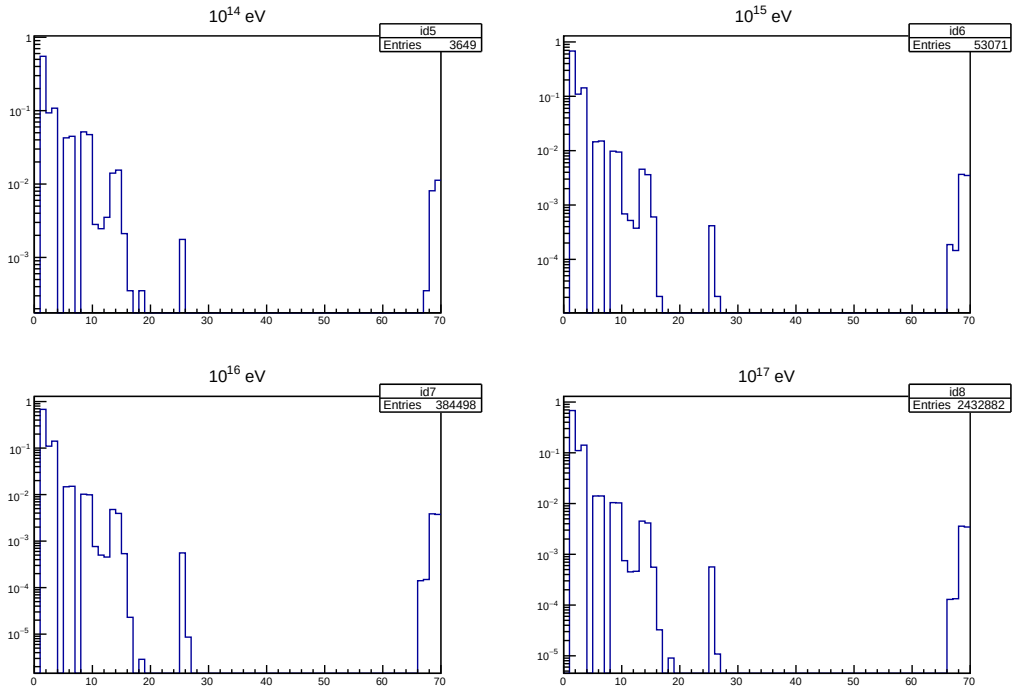

Number	Type of particle
1	Photon
2-3	Electrons
5-6	Muons
7-9	Pions
10-13,16	Kaons
13,25	(Anti) Neutron
14-15	(Anti) Proton
66-69	Neutrino's

Table 5.2: Particle identification

5.3 Charm

Now we look at the impact of charm in the transverse momentum distribution of muons, photons+electrons and neutrino's

In table 5.3 are the number of charm particles who are the mother or grandmother of a muon. For every order of magnitude the primairy particle increases the number of charm particles in the shower increases with a factor of 5.

Primairy particle energy (eV)	Number of charm particles	Average
10^{14}	107	0.21
10^{15}	215	1.08
10^{16}	503	5.03
10^{17}	1092	21.84
10^{18}	1291	129.1

Table 5.3: Number of charm particles in the showers

Fig 5.4 are the momenta distribution of two simulations of showers initiated by a 10^{14} eV proton with and without charm. For all three particle types the number of produced particles has increased. Also for the muons and neutrino's the mean momentum has increased while the photon and electron momenum decreases.

In Fig 5.5 the primairy particle energy is 10^{15} eV. Again the number of particles in the shower rises due to charm. However now both the muon and photon+electron momentum is lowered. Neutrino momentum is still increased by charm.

For a 10^{16} eV shower in Fig 5.6 the momentum and number of particles has increased for all three particle types.

Figure 5.7 is the 10^{17} eV shower data. Again the momentum of muons, neutrino's and photon+electron has increased. On the other hand the number of particles has decreased.

Last is the 10^{18} eV shower in Fig 5.8. Here there is a very clear increase in the number of particles for muons, photons, electrons and neutrino's. And the momentum for all three has decreased.

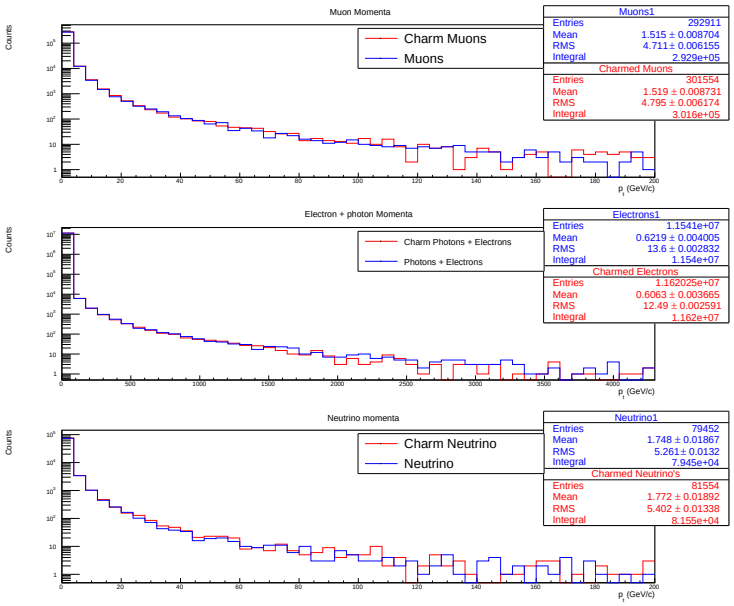

Figure 5.4: 10^{14} eV primairy particle

Figure 5.5: 10^{15} eV primairy particle

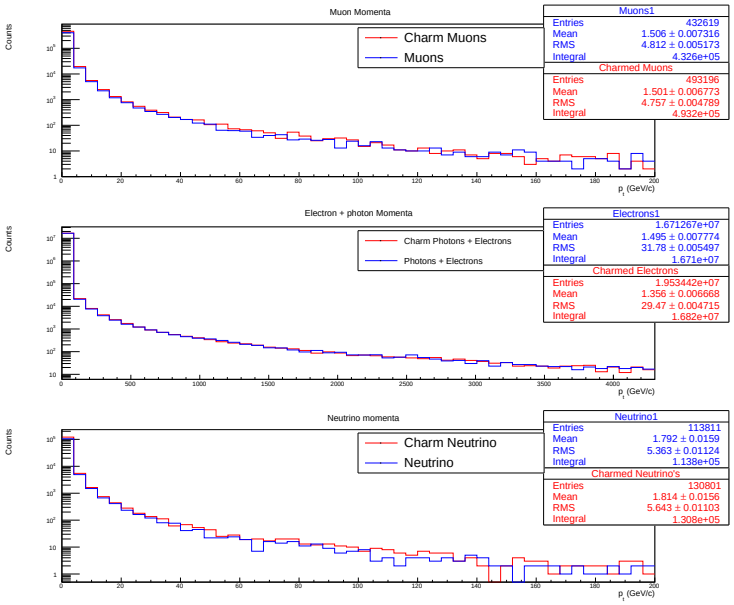

Figure 5.6: 10^{16} eV primairy particle

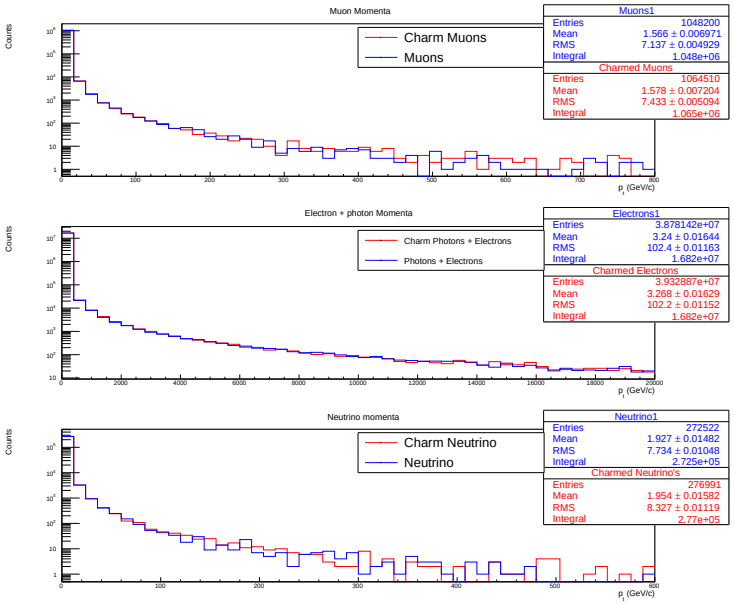

Figure 5.7: 10^{17} eV primairy particle

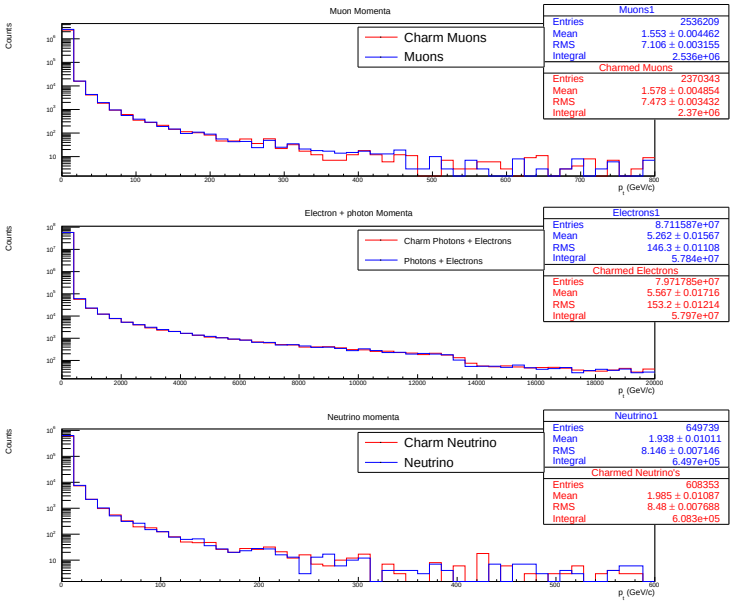

Figure 5.8: 10^{18} eV primairy particle

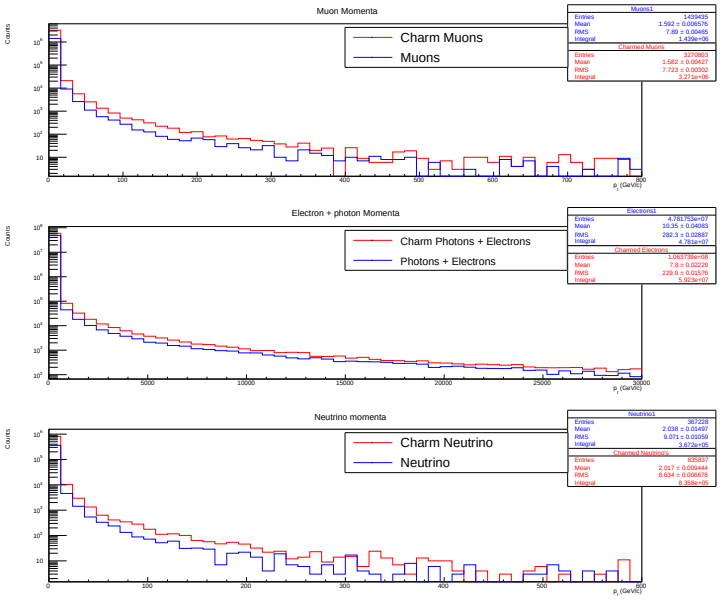

For easy comparison between diferent showers I will summarize important facts in plot as a function of the primairy particle energy. First in Fig 5.9 are the mean momentum of muons, photons+electrons and neutrino's for both shower with and without charm.

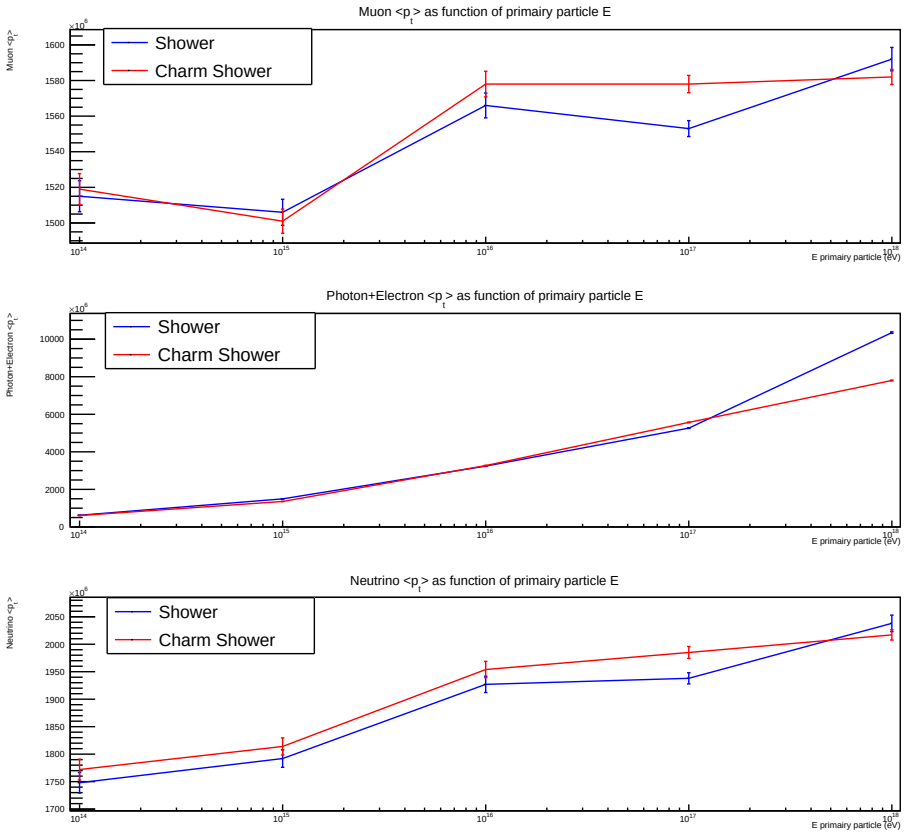

Figure 5.9: Mean Momentum for muons, photon+electron and neutrino's for shower energies from 10^{14} to 10^{18} eV

In figure 5.10 are the fractions of particles being muons, photons+electrons and neutrino's. This is the number of particles divided by the total number of particles in the shower. From this it is visible both Charm and a higher primairy particle energy result in the same effect. Namely muons and neutrino's become more aboundand while the number of photons and electrons goes down. Finally in Fig 5.11 is the total number of particles produced in the different showers.

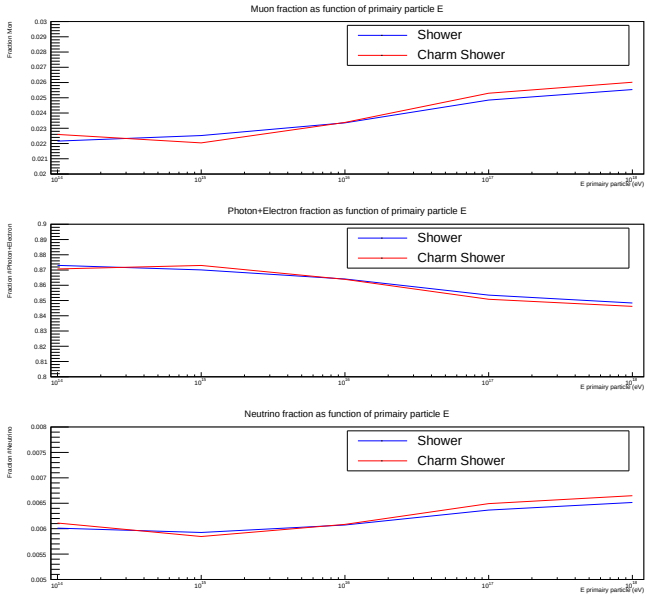

Figure 5.10: Fraction of muons, photon+electrons and neutrino's.

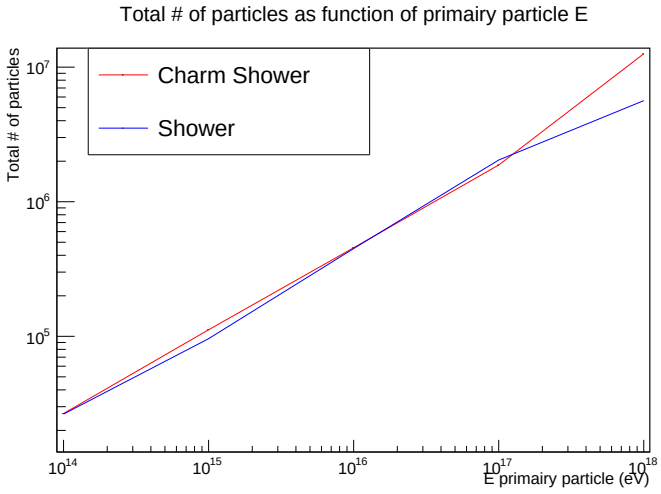

Figure 5.11: Total number of particles.

5.4 Link to the HiSparc experiment

The last thing to be adressed is the link to the HiSparc experiment. As mentioned before it is possible to fit data from collected by HiSparc stations and determain the quantitaty $\frac{Landau}{Exponential}$. This number should be representative of the ratio of muon to photon+electron momenta of the particles going through the detector.

Using the data from the CORSIKA simulations we can also calculate the ratio of muon to photon+electron momentum. From this data we can look at two things. First of the dependance of this ratio on the primairy particle energy. Secondly the dependence of the ratio with and without allowing Charm to be produced.

The importance of this is fairly straight forward. This answers the all important question:*"Can we measure the influence ofthe charm quark?"*

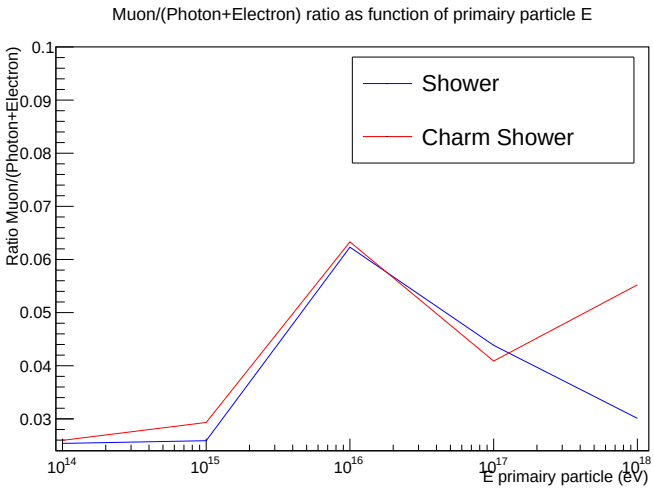

As is visible from Fig 5.both the inclusion of Charm and a higher primairy particle energy shift this ratio to slightly higher values. Except at 10^{17} where there is a drop

For comparision in table 5.3 is the calculated ratio of $\frac{Landau}{Exponential}$ from 5 days of HiSparc data

Date	Ratio
$2015-09-01$	0.61
$2015-09-02$	0.59
$2015-09-03$	0.59
$2015-09-04$	0.61
$2015-09-05$	0.63

Table 5.4: Ratio of fitted $\frac{Landau}{Exponential}$ of 5 days of data, taken from the HiSparc station 501 at NiKHEF

From the HiSparc data this ratio is around 0.6 In the simulations the ratio is somewhere around 0.03.

Chapter 6

Conclusion

In the search of the impact of Charm quarks on high energy cosmic rays some important features appeared. In summary, once again.

- The number of particles produced when Charm is enables is significantly higher then without Charm.
- Mean p_t is higher with Charm for muons and neutrino's.
- Mean p_t is lower with Charm for photons+electrons.
- At higher energies the difference due to Charm becomes larger.
- The number of particles produced when Charm is enables is significantly higher then without Charm.
- The fraction of muons and neutrino's becomes larger with Charm.
- The fraction photon+electrons goes down with Charm.
- The observable quantity $\mu/(\gamma + e)$ is higher.

Chapter 7

Discussion

What is important to keep in mind is the fact that this holds for EAS produced by primairy particles at 1 kilometer above sea level. It is extreamly unlikely a high energy cosmic particle reaches this altitude without interaction at all with the atmosphere. On the other hand it is clear Charm already has a large influence on even a short longitudinal scale.

In an EAS the only particles reaching sealevel are photons, electrons, muons and neutrino's. In my simulations there still where large numbers of pions kaons and other instable particles, which provide a significant contribution to the muon and neutrino parts of a shower when decaying. Seeing high energy particles have a longer lifetime it is expectable these particles will push muon and neutrino momentum to higher values if the simulation would have a shower start at higher altitudes. At the same time the high energy photons and electrons also interact with the atmosphere, losing energy in the process. So it is not unlikely the ratio of muon/photon electron momentum to actually be much larger then it is resulting from simulation.

What is clear is that there is that the shower development changes when charm is introduced. Unfortunatly how this converts to differences in the end result is not jet fully clear.It is hard to draw conclusion because different shower show different results.

Chapter 8

Appendix

8.1 x-y plane

There are the x-y planes for different types of particles, namely muons, photons+electrons and neutrino's. From these it is visible the muons and neutrion's have a smaller spread then the photons and electrons.

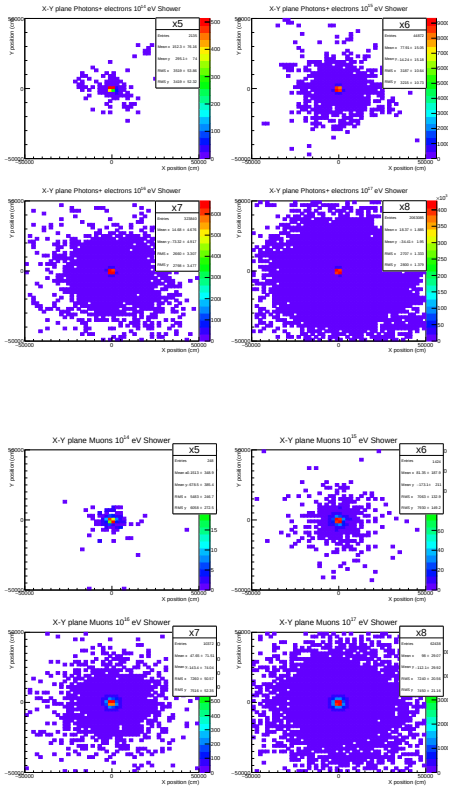

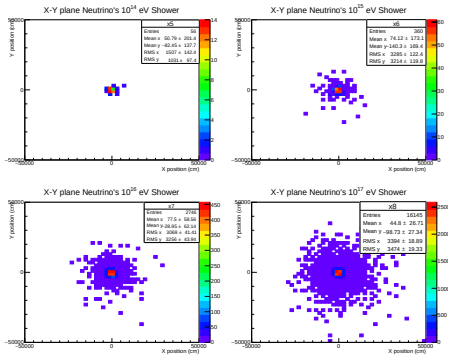
X-Y plane Neutrino's 10^{14} eV Shower
X-Y plane Neutrino's 10^{15} eV Shower
X-Y plane Neutrino's 10^{16} eV Shower
X-Y plane Neutrino's 10^{17} eV Shower
X position (cm)
Y position (cm)

8.2 CORSIKA Data cards

This is the full input used to stear the CORSIKA simulation

```
RUNNR 10901 run number
EVTNR 1 number of first shower event
NSHOW 3 number of showers to generate
PRMPAR 14 particle type of prim. particle
ESLOPE -2.7 slope of primary energy spectrum
ERANGE 1.E9 1.E9 energy range of primary particle
THETAP 20. 20. range of zenith angle (degree)
PHIP -180. 180. range of azimuth angle (degree)
SEED 123 0 0 seed for 1. random number sequence
SEED 456 0 0 seed for 2. random number sequence
OBSLEV 0 observation level (in cm)
FIXHEI 100000 2 Height of first interaction
MAGNET 20.0 42.8 magnetic field centr. Europe
ECUTS 0.3 0.3 0.003 0.003 energy cuts for particles
MUADDI T additional info for muons
MUMULT T muon multiple scattering angle
ELMFLG T T em. interaction flags (NKG,EGS)
STEPFC 1.0 mult. scattering step length fact.
RADNKG 200.E2 outer radius for NKG lat.dens.distr.
ECTMAP 1.E4 cut on gamma factor for printout
MAXPRT 1 max. number of printed events
DIRECT ./Definitief/ output directory
USER you user
DEBUG F 6 F 1000000 debug flag and log.unit for out
SIGMAQ 0 0 0 0
PROPAQ 1
PLOTSH F
EXIT
```

Bibliography

[1] Pierre Auger, Paul Ehrenfest, Roland Maze, Jean Daudin, and Robley A Fréon. Extensive cosmic-ray showers. *Reviews of Modern Physics*, 11(3-4):288, 1939.

[2] A Bueno and A Gascon. Corsika implementation of heavy quark production and propagation in extensive air showers. *Computer Physics Communications*, 185(2):638–650, 2014.

[3] D Fokkema. *The HiSPARC Experiment, data acquisition and reconstruction of shower direction.* PhD thesis, Dissertation, Universiteit Twente, 2012.

[4] Alberto Gascón Bravo. *Heavy Quark simulation and identification at the Pierre Auger Observatory.* Universidad de Granada, 2014.

[5] Kenneth Greisen. Cosmic ray showers. *Annual Review of Nuclear Science*, 10(1):63–108, 1960.

[6] D Heck and T Pierog. Corsika users guide, 2013.

[7] Dieter Heck, G Schatz, J Knapp, T Thouw, and JN Capdevielle. Corsika: A monte carlo code to simulate extensive air showers. Technical report, 1998.

[8] Maurizio Spurio. Particles and astrophysics, 2014.

[9] Todor Stanev. *High energy cosmic rays.* Springer Science Business Media, 2010.

[10] JW Van Holten. Hisparc a view from the bottom. 2005.